A first-order qSV-wave propagator in 2D VTI media

He Liu and Kris Innanen

Mar 13, 2020

NSERC CRSNG
UNIVERSITY OF CALGARY
FACULTY OF SCIENCE
Department of Geoscience

Outline

- Motivation
- Methodology
- Synthetic Examples
- Conclusions

Motivation

- Dellinger and Etgen (1990) proposed to separate P- and S-wavefields with wavenumber-domain operators (polarization vector) in homogeneous media.
- Yan and Sava (2009, 2011) proposed to separate P- and S-wavefields with space-domain operators, which can be used in heterogeneous media.
- Other than directly separate P- and S-waves from full elastic waves, some researchers have tried to solve it by the forward simulation of pure P- and S-waves (Zhang et al., 2007; Cheng and Kang, 2013, 2016).

Motivation

- Zhang et al. (2007) proposed to simulate separated P- and S-waves with fully decoupled first-order P- and S-wave equations using staggered-grid finite-difference method.
- Cheng and Kang (2016) proposed to split wavefield separation into a two-steps procedure, which is an alternative approach to simulate separated S-waves using modified second-order elastic wave equations in anisotropic media.
- Adopt staggered-grid scheme (Virieux, 1984; 1986) for better accuracy and efficiency.
- Adopt first-order Hybrid-PML (Zhang et al., 2014) to achieve better performance and stability in the models with extreme anisotropy.

First-order propagator of qSV-waves in 2D VTI media

Based on Helmholtz theory (Aki and Richards, 2002), a wavefield vector **U** = {Ux, Uz} in isotropic media can be decomposed into P-wavefield (curl-free) and S-wavefield (divergence-free)

$$U = U^P + U^S, \tag{1}$$

In isotropic media, scalar S-waves can be separated from displacement wavefield **U** by applying a curl operation

$$\tilde{U}^S = i\, K \times \tilde{U}. \tag{2}$$

In anisotropic media, equation (2) can be rewritten as

$$\tilde{U}^{SV} = i\, a^{qP} \times \tilde{U} \tag{3}$$

where $a^{qP} = (a_x^{qP}, a_z^{qP})^T$ is the polarization vector of qP-mode waves.

For heterogeneous models, this separation procedure need to be performed using nonstationary space domain operators (Yan and Sava, 2009).

First-order propagator of qSV-waves in 2D VTI media

Cheng and Kang (2016) proposed to split this separation procedure into a two-steps scheme.

First, project the original qSV-wavefield onto isotropic references of local polarization direction through the introduction of a similarity transform to Christoffel matrix G

$$\tilde{G}_{qSV} = M_{SV}\ G\ M_{SV}^{-1} \tag{4}$$

Where

$$M_{SV} = \begin{bmatrix} k_x\ k_z & 0 \\ 0 & -k_x^2 \end{bmatrix} \tag{5}$$

According to the elastic matrix of 2D VTI medium,

$$C = \begin{bmatrix} C_{11} & C_{13} & \\ C_{13} & C_{33} & \\ & & C_{44} \end{bmatrix} \tag{6}$$

First-order propagator of qSV-waves in 2D VTI media

Christoffel matrix $\tilde{G}$ has the form as below:

$$\tilde{G} = \begin{bmatrix} C_{11}\ k_x^2 + C_{44}\ k_z^2 & (C_{13} + C_{44})\ k_x\ k_z \\ (C_{13} + C_{44})\ k_x\ k_z & C_{44}\ k_x^2 + C_{33}\ k_z^2 \end{bmatrix}. \quad (7)$$

After the similarity transform of Christoffel matrix,

$$\tilde{G}_{qSV} = \begin{bmatrix} C_{11}\ k_x^2 + C_{44}\ k_z^2 & -(C_{13} + C_{44})\ k_z^2 \\ -(C_{13} + C_{44})\ k_x^2 & C_{44}\ k_x^2 + C_{33}\ k_z^2 \end{bmatrix} \quad (8)$$

In this way, Christoffel equation of qSV-waves is derived as below:

$$\tilde{G}^{qSV} \tilde{U}^{qSV} = \rho\omega^2 \tilde{U}^{qSV}. \quad (9)$$

Through inverse Fourier transform of equation (9), second-order pseudo-pure-qSV-mode wave equations can be obtained:

$$\rho \frac{\partial^2 \overline{U}^{qSV}}{\partial t^2} = \overline{GU}^{qSV}. \quad (10)$$

First-order propagator of qSV-waves in 2D VTI media

The second-order qSV-mode wave equation (10), can be expressed as below:

$$\rho\frac{\partial^2 u_x}{\partial t^2} = C_{11}\frac{\partial^2 u_x}{\partial x^2} + C_{44}\frac{\partial^2 u_x}{\partial z^2} - (C_{13}+C_{44})\frac{\partial^2 u_z}{\partial z^2} \qquad (11)$$

$$\rho\frac{\partial^2 u_z}{\partial t^2} = C_{33}\frac{\partial^2 u_z}{\partial z^2} + C_{44}\frac{\partial^2 u_z}{\partial x^2} - (C_{13}+C_{44})\frac{\partial^2 u_x}{\partial x^2}.$$

The scalar wavefield **U** still contains some weak residual qP-waves. So equation 11 is called a pseudo-pure-qSV-wave equations (Cheng and Kang, 2016).

Virieux (1984, 1986) proposed to adopt staggered-grid scheme in the velocity-stress elastic wave equations for better efficiency and accuracy .

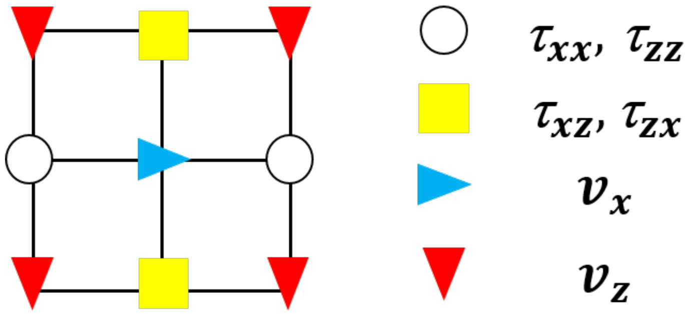

Fig 1. 2D Staggered grid

First-order propagator of qSV-waves in 2D VTI media

First, we introduce velocity fields vx and vz as intermediate variables and let

$$\frac{\partial\ u_x}{\partial t} = v_x \qquad (12)$$

$$\frac{\partial\ u_z}{\partial t} = v_z$$

Equation (12) keeps the same relationship between displacement and velocity fields as in original elastic wave equations (Virieux, 1986).

First-order propagator of qSV-waves in 2D VTI media

First, we introduce velocity fields vx and vz as intermediate variables and let

$$\frac{\partial\ u_x}{\partial t} = v_x \qquad (12)$$
$$\frac{\partial\ u_z}{\partial t} = v_z$$

Equation (12) keeps the same relationship between displacement and velocity fields as in original elastic wave equations.

For qSV-mode wave equation (11), we further introduce variables $\sigma_{xx},\ \sigma_{zz},\ \sigma_{xz},\ \sigma_{zx}$ (Liu et al., 2018)

$$\rho\frac{\partial\sigma_{xx}}{\partial t} = C_{11}\frac{\partial\ v_x}{\partial x} \qquad (13)$$
$$\rho\frac{\partial\sigma_{zz}}{\partial t} = C_{33}\frac{\partial\ v_z}{\partial z}$$
$$\rho\frac{\partial\sigma_{xz}}{\partial t} = C_{44}\frac{\partial\ v_x}{\partial z} - (C_{13} + C_{44})\frac{\partial\ v_z}{\partial z}$$
$$\rho\frac{\partial\sigma_{zx}}{\partial t} = C_{44}\frac{\partial\ v_z}{\partial x} - (C_{13} + C_{44})\frac{\partial\ v_x}{\partial x}$$

First-order propagator of qSV-waves in 2D VTI media

Then we substitute equation (13) into equation (11),

$$\rho \frac{\partial\ v_x}{\partial t} = \frac{\partial\ \sigma_{xx}}{\partial x} + \frac{\partial\ \sigma_{xz}}{\partial z} \tag{14}$$
$$\rho \frac{\partial\ v_z}{\partial t} = \frac{\partial\ \sigma_{zx}}{\partial x} + \frac{\partial\ \sigma_{zz}}{\partial z}$$

Wave modes can also be separated from velocity and stress fields (Zhang and McMechan, 2010) .

First-order propagator of qSV-waves in 2D VTI media

Then we substitute equation (13) into equation (11), we get:

$$\rho\frac{\partial\, v_x}{\partial t} = \frac{\partial\, \sigma_{xx}}{\partial x} + \frac{\partial\, \boxed{\sigma_{xz}}}{\partial z}$$
$$\rho\frac{\partial\, v_z}{\partial t} = \frac{\partial\, \boxed{\sigma_{zx}}}{\partial x} + \frac{\partial\, \sigma_{zz}}{\partial z} \qquad (14)$$

Wave modes can also be separated from velocity and stress fields (Zhang and McMechan, 2010) .

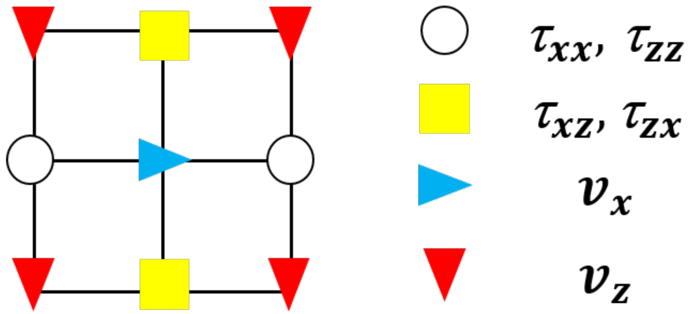

Fig 1. 2D Staggered Grid

vx and vz are not distributed at the same nodes, therefore vz field needs to be phase shifted. Alternatively, corresponding vz field could be averaged by 4 vz fields surrounding the vx field.

First-order propagator of qSV-waves in 2D VTI media

Applying the Thomsen notation (Thomsen, 1986):

$$C_{11} = (1+2\epsilon)\rho\, v_{p0}^2$$

$$C_{33} = \rho\, v_{p0}^2$$

$$C_{44} = \rho\, v_{s0}^2$$

$$v_{pn} = v_{p0}\sqrt{(1+2\delta)}$$

$$(C_{33}+C_{44})^2 = \rho^2(v_{p0}^2 - v_{s0}^2)(v_{pn}^2 - v_{s0}^2)$$

First-order propagator of qSV-waves in 2D VTI media

Applying the Thomsen notation (Thomsen, 1986):

$$
\begin{aligned}
C_{11} &= (1+2\epsilon)\rho\ v_{p0}^2 \\
C_{33} &= \rho\ v_{p0}^2 \\
C_{44} &= \rho\ v_{s0}^2 \\
v_{pn} &= \ v_{p0}\sqrt{(1+2\delta)} \\
(C_{33}+C_{44})^2 &= \rho^2(\ v_{p0}^2 -\ v_{s0}^2)(\ v_{pn}^2 -\ v_{s0}^2)
\end{aligned}
$$

The first-order qSV-wave equations can be rewritten as below:

$$
\begin{aligned}
\rho\frac{\partial\sigma_{xx}}{\partial t} &= (1+2\epsilon)\rho\ v_{p0}^2\frac{\partial\ v_x}{\partial x} \\
\rho\frac{\partial\sigma_{zz}}{\partial t} &= \rho\ v_{p0}^2\frac{\partial\ v_z}{\partial z} \\
\rho\frac{\partial\sigma_{xz}}{\partial t} &= \rho\ v_{s0}^2\frac{\partial\ v_x}{\partial z} - \sqrt{\rho^2(\ v_{p0}^2 -\ v_{s0}^2))(\ v_{pn}^2 -\ v_{s0}^2)}\frac{\partial\ v_z}{\partial z} \\
\rho\frac{\partial\sigma_{zx}}{\partial t} &= \rho\ v_{s0}^2\frac{\partial\ v_z}{\partial x} - \sqrt{\rho^2(\ v_{p0}^2 -\ v_{s0}^2))(\ v_{pn}^2 -\ v_{s0}^2)}\frac{\partial\ v_x}{\partial x} \\
\rho\frac{\partial\ v_x}{\partial t} &= \frac{\partial\ \sigma_{xx}}{\partial x} + \frac{\partial\ \sigma_{xz}}{\partial z} \\
\rho\frac{\partial\ v_z}{\partial t} &= \frac{\partial\ \sigma_{zx}}{\partial x} + \frac{\partial\ \sigma_{zz}}{\partial z}
\end{aligned}
$$

First-order propagator of qSV-waves in 2D VTI media

Applying the Thomsen notation (Thomsen, 1986):

$$C_{11} = (1+2\epsilon)\rho\, v_{p0}^2$$
$$C_{33} = \rho\, v_{p0}^2$$
$$C_{44} = \rho\, v_{s0}^2$$
$$v_{pn} = v_{p0}\sqrt{(1+2\delta)}$$
$$(C_{33}+C_{44})^2 = \rho^2(\, v_{p0}^2 - \, v_{s0}^2)(\, v_{pn}^2 - \, v_{s0}^2)$$

The first-order qSV-wave equations can be rewritten as below:

$$\rho\frac{\partial\sigma_{xx}}{\partial t} = (1+2\epsilon)\rho\, v_{p0}^2\frac{\partial\, v_x}{\partial x}$$
$$\rho\frac{\partial\sigma_{zz}}{\partial t} = \rho\, v_{p0}^2\frac{\partial\, v_z}{\partial z}$$
$$\rho\frac{\partial\sigma_{xz}}{\partial t} = \rho\, v_{s0}^2\frac{\partial\, v_x}{\partial z} - \sqrt{\rho^2(\, v_{p0}^2 - \, v_{s0}^2))(\, v_{pn}^2 - \, v_{s0}^2)}\frac{\partial\, v_z}{\partial z}$$
$$\rho\frac{\partial\sigma_{zx}}{\partial t} = \rho\, v_{s0}^2\frac{\partial\, v_z}{\partial x} - \sqrt{\rho^2(\, v_{p0}^2 - \, v_{s0}^2))(\, v_{pn}^2 - \, v_{s0}^2)}\frac{\partial\, v_x}{\partial x}$$
$$\rho\frac{\partial\, v_x}{\partial t} = \frac{\partial\,\sigma_{xx}}{\partial x} + \frac{\partial\,\sigma_{xz}}{\partial z}$$
$$\rho\frac{\partial\, v_z}{\partial t} = \frac{\partial\,\sigma_{zx}}{\partial x} + \frac{\partial\,\sigma_{zz}}{\partial z}$$

Besides, the first-order Hybrid-PML (Zhang et al., 2014) can be directly implemented in this first-order finite difference algorithm. The stretching factor is expressed as:

$$s_x = \frac{d_x + m_{x/z}d_z}{\alpha_x + i\omega} \qquad (17)$$

Correction of projection deviation of qSV-waves

Similarity transform of Christoffel matrix

$$\tilde{G}_{qSV} = M_{SV} \; G \; M_{SV}^{-1} \tag{4}$$

This procedure equals to project the wavefield on the isotropic references

$$\tilde{U}^S = i \; K \times \tilde{U}. \tag{2}$$

Correction of projection deviation of qSV-waves

Similarity transform of Christoffel matrix

$$\tilde{G}_{qSV} = M_{SV}\ G\ M_{SV}^{-1} \tag{4}$$

This procedure equals to project the wavefield on the isotropic references

$$\tilde{U}^{S} = i\ K \times \tilde{U}. \tag{2}$$

- a partial separation is achieved during wavefield simulation.
- there will still be some residual qP-wave energy in the synthetic wavefields.
- separation operators in anisotropic media need to be normalized by the separation operators in isotropic media to obtain the space-domain deviation operators (Cheng and Kang, 2016).

To achieve a complete wavefield separation, apply space-domain deviation operators to the synthetic wavefields.

Correction of projection deviation of qSV-waves

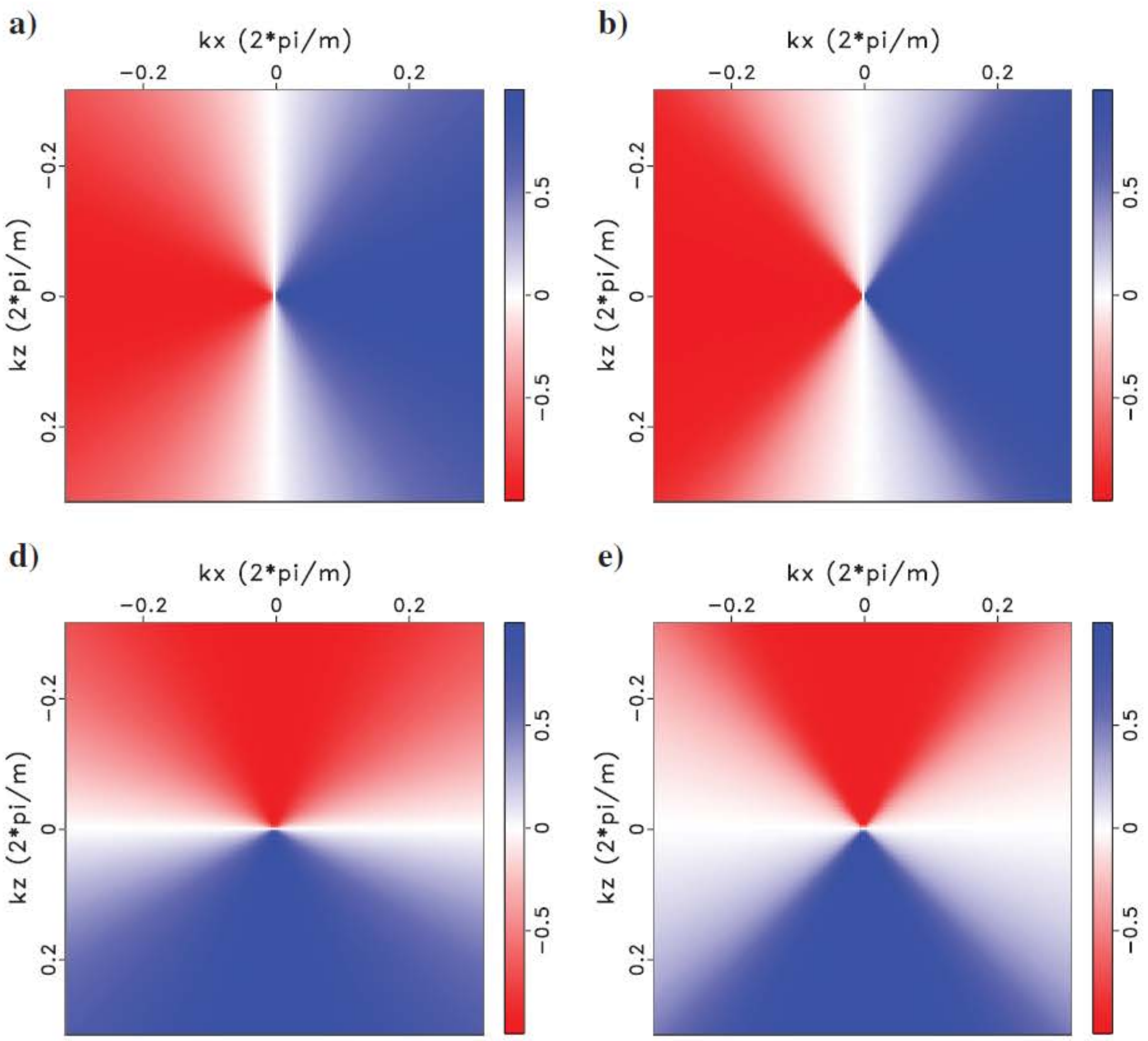

Dellinger and Etgen, 1990

Figure 1. Wavenumber-domain operators of projection onto isotropic (reference) and anisotropic polarization vectors of qP-waves, and wavenumber-domain deviation operators in a 2D homogeneous VTI medium: k (left), ap (middle), and Ep (right); Top: x-component, Bottom: z-component.

Correction of projection deviation of qSV-waves

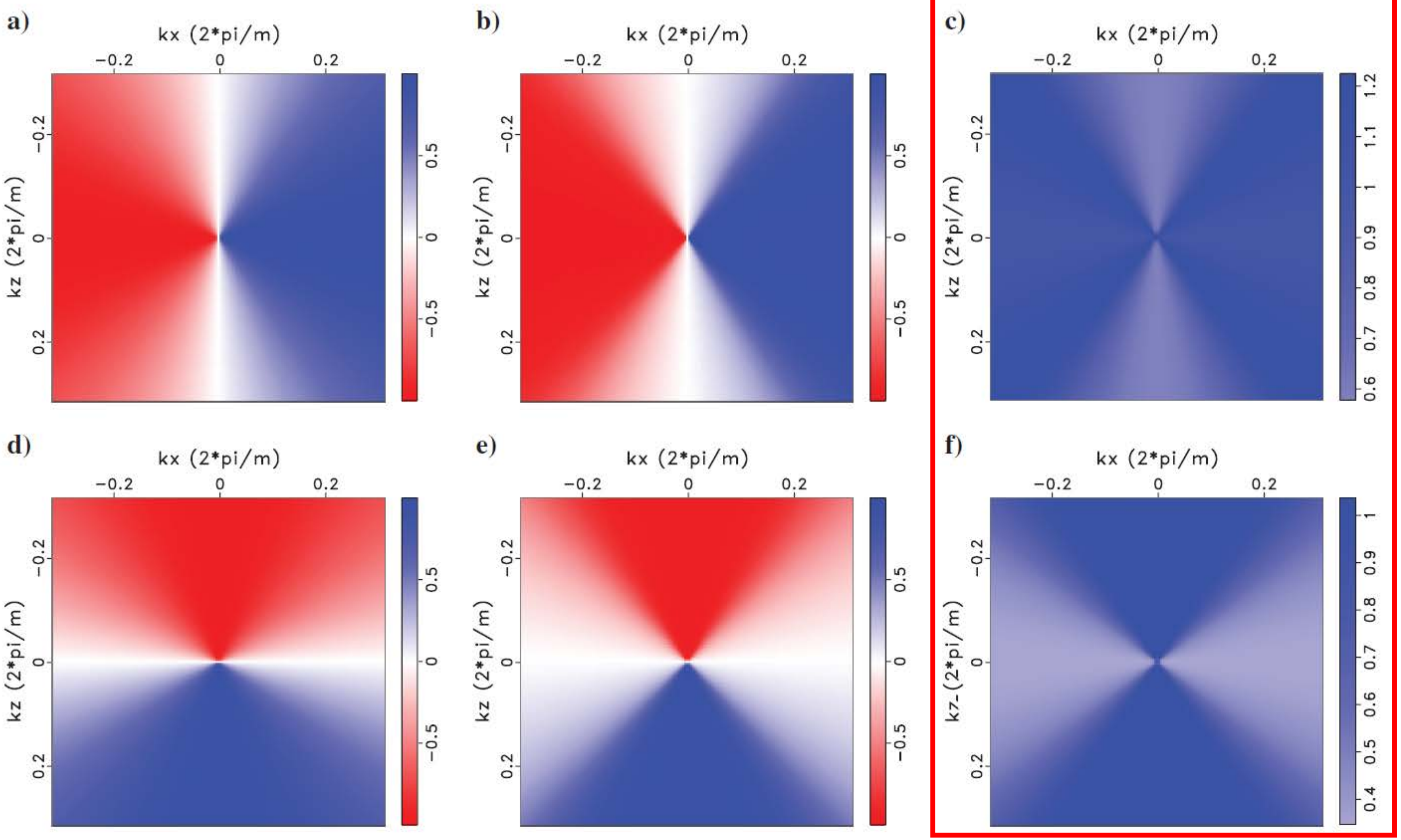

Dellinger and Etgen, 1990

Cheng and Kang, 2016

Figure 1. Wavenumber-domain operators of projection onto isotropic (reference) and anisotropic polarization vectors of qP-waves, and wavenumber-domain deviation operators in a 2D homogeneous VTI medium: k (left), ap (middle), and Ep (right); Top: x-component, Bottom: z-component.

Correction of projection deviation of qSV-waves

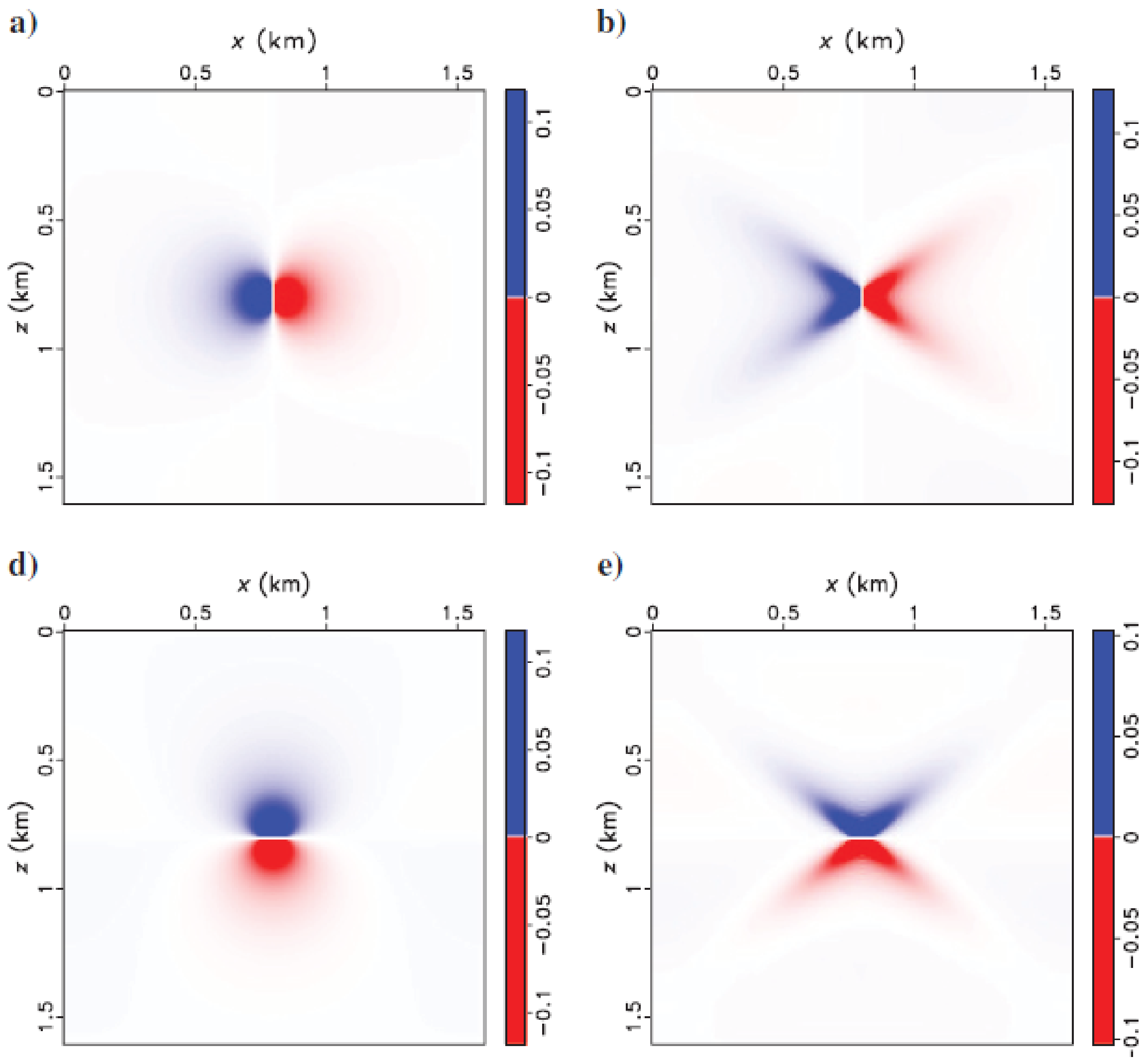

Yan and Sava, 2009

Figure 2. Space-domain operators of projecting onto isotropic (left) and anisotropic (middle) polarization vectors, and the corresponding deviation operators (right): Top: x-component, Bottom: z-component.

Correction of projection deviation of qSV-waves

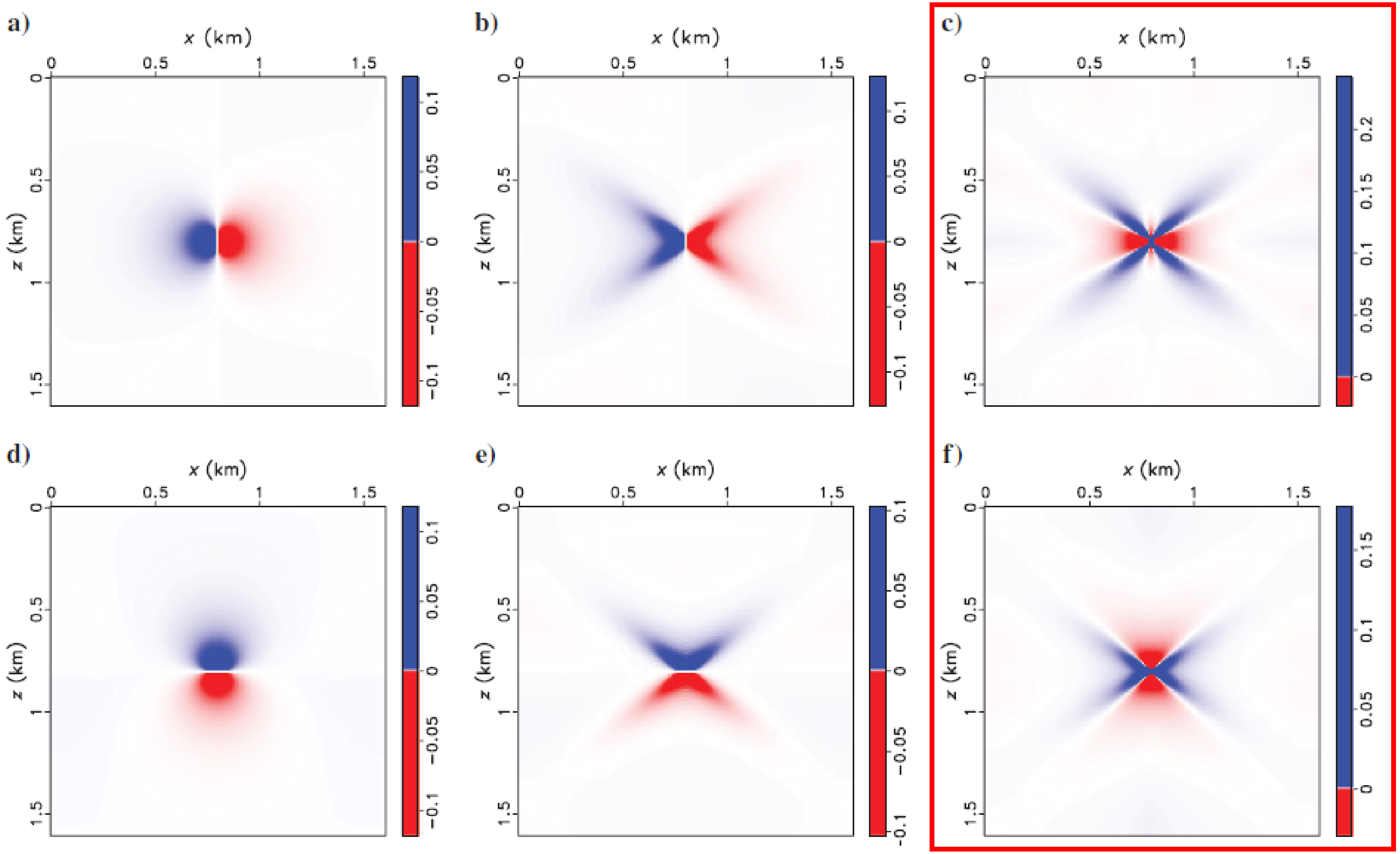

Yan and Sava, 2009

Cheng and Kang, 2016

Figure 2. Space-domain operators of projecting onto isotropic (left) and anisotropic (middle) polarization vectors, and the corresponding deviation operators (right): Top: x-component, Bottom: z-component.

Simulation examples of separated scalar qSV-waves

Homogeneous isotropic medium

Model size : 2 km*2 km
Density :   2500 kg/m3
Vp: 4000 m/s
Vs: 2300 m/s

a

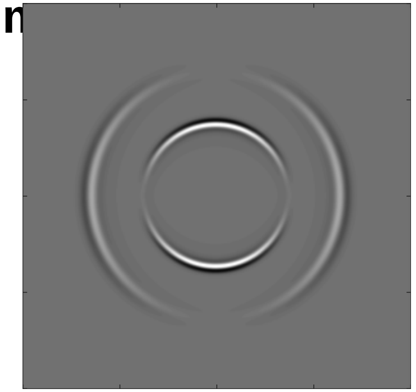

c

e

b

d

For isotropic media, this algorithm directly produces scalar SV-waves.

FIG. 3. Synthetic wavefields in an isotropic medium: a) x- and b) z-component simulated by original elastic wave equations; c) x- and d) z-components simulated by first-order pseudo-pure-mode qSV-wave equations; e) separated scalar qSV-wave field.

Simulation examples of separated scalar qSV-waves

Homogeneous VTI medium with weak anisotropy

v_{p0} = 3000m/s, ϵ = 0.1
v_{s0} = 1500m/s, δ = 0.05
Cheng and Kang (2013, 2016)

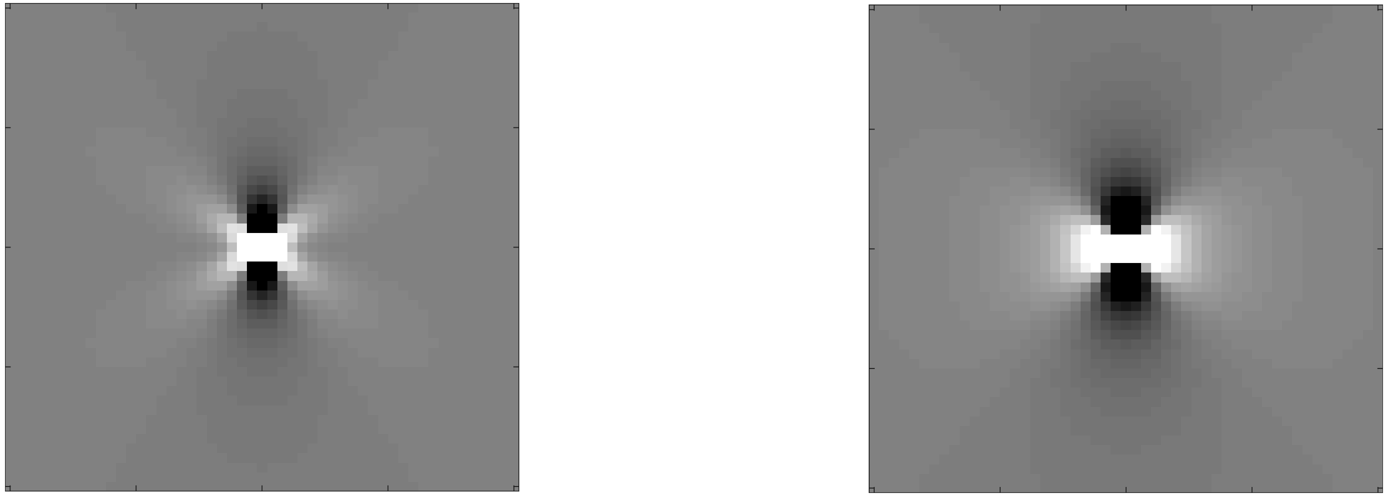

FIG. 3. Space-domain deviation operators.

Simulation examples of separated scalar qSV-waves

Homogeneous VTI medium with weak anisotropy

v_{p0} = 3000m/s, ϵ = 0.1
v_{s0} = 1500m/s, δ = 0.05
Cheng and Kang (2013, 2016)

a

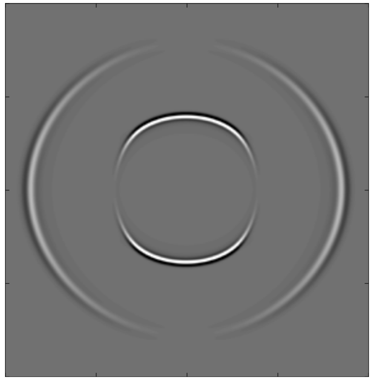

c

e

b

d

f

the summation produces scalar wavefields dominant of qSV-wave energy.

FIG. 7. Synthetic wavefields in a VTI medium with weak anisotropy: a) x- and b) z-component simulated by original elastic wave equations; c) x- and d) z-component simulated by first-order pseudo-pure-mode qSV-wave equations; e) pseudo-pure-mode scalar qSV-wave field; f) separated scalar qSV-wave field.

Simulation examples of separated scalar qSV-waves

Homogeneous VTI medium with weak anisotropy

v_{p0} = 3000m/s, ϵ = 0.1
v_{s0} = 1500m/s, δ = 0.05
Cheng and Kang (2013, 2016)

The summation produces scalar wavefields dominant of qSV-wave energy.

Residual qP-wave

a

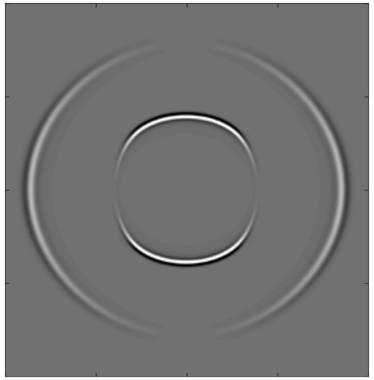

c

e

b

d

f

FIG. 7. Synthetic wavefields in a VTI medium with weak anisotropy: a) x- and b) z-component simulated by original elastic wave equations; c) x- and d) z-component simulated by first-order pseudo-pure-mode qSV-wave equations; e) pseudo-pure-mode scalar qSV-wave field; f) separated scalar qSV-wave field.

Simulation examples of separated scalar qSV-waves

Homogeneous VTI medium with strong anisotropy

c_{11} = 23.87 GPa,
c_{33} = 15.33 GPa,
c_{13} = 9.79 GPa,
c_{44} = 2.77 Gpa,
ρ = 2500 kg/m^3
(Tang, 2004)

a

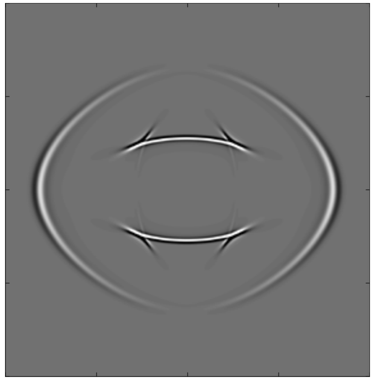

c

e

b

d

f

FIG. 8. Synthetic wavefields in a VTI medium with strong anisotropy: a) x- and b) z-component simulated by original elastic wave equations; c) x- and d) z-component simulated by first-order pseudo-pure-mode qSV-wave equations; e) pseudo-pure-mode scalar qSV-wave field; f) separated scalar qSV-wave field.

Simulation examples of separated scalar qSV-waves

Homogeneous VTI medium with strong anisotropy

c_{11} = 23.87 GPa,
c_{33} = 15.33 GPa,
c_{13} = 9.79 GPa,
c_{44} = 2.77 Gpa,
ρ = 2500 kg/m^3
(Tang, 2004)

a

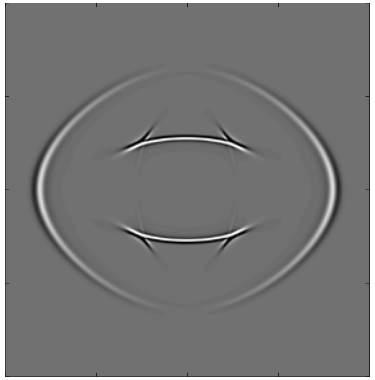

c

e

Residual qP-wave

b

d

f

FIG. 8. Synthetic wavefields in a VTI medium with strong anisotropy: a) x- and b) z-component simulated by original elastic wave equations; c) x- and d) z-component simulated by first-order pseudo-pure-mode qSV-wave equations; e) pseudo-pure-mode scalar qSV-wave field; f) separated scalar qSV-wave field.

Simulation examples of separated scalar qSV-waves

Performance of Hybrid-PML implemented in this algorithm

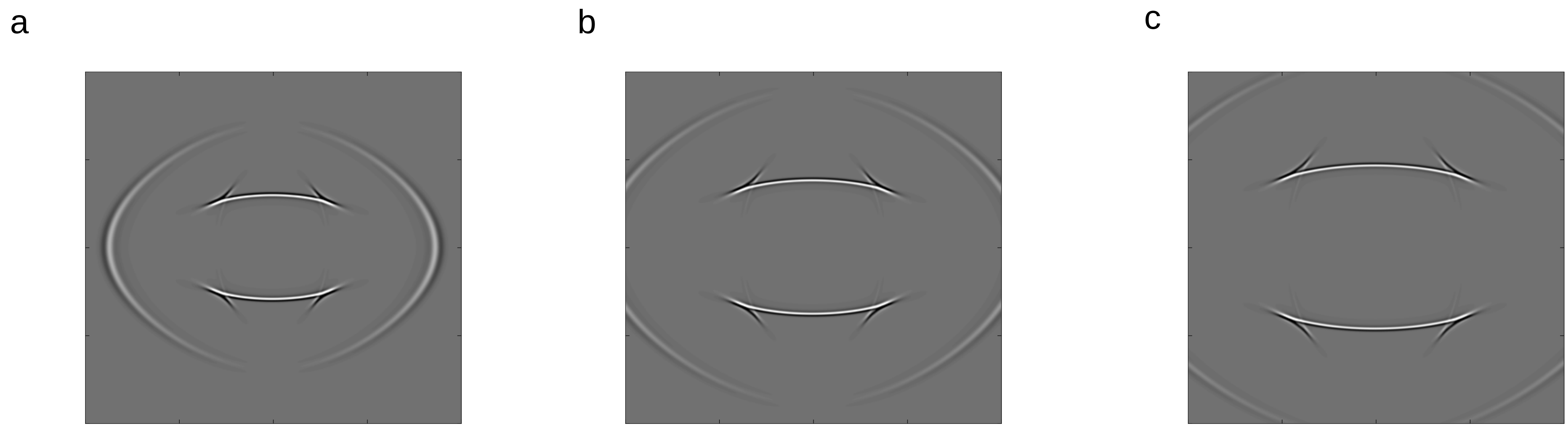

FIG. 9. Snapshots of x-component simulated by first-order pseudo-pure-mode qSV-wave equations in a VTI medium with strong anisotropy: a) 320 ms, b) 400 ms and c) 480 ms, respectively.

Simulation examples of separated scalar qSV-waves

Heterogeneous bilayer VTI media

a

c

e

First layer:
strongly anisotropic medium

b

d

f

Second layer:
weakly anisotropic medium

FIG. 10. Synthetic wavefields in a layered VTI model with strong anisotropy in the first layer and weak anisotropy in the second layer: a) x- and b) z-component simulated by original elastic wave equations; c) x- and d) z-component simulated by first-order pseudo-pure-mode qSV-wave equations; e) pseudo-pure-mode scalar qSV-wave field; f) separated scalar qSV-wave field.

Simulation examples of separated scalar qSV-waves

Heterogeneous bilayer VTI media

First layer:
strongly anisotropic medium

Second layer:
weakly anisotropic medium

a

c

e

qP-wave

converted P

b

d

f

FIG. 10. Synthetic wavefields in a layered VTI model with strong anisotropy in the first layer and weak anisotropy in the second layer: a) x- and b) z-component simulated by original elastic wave equations; c) x- and d) z-component simulated by first-order pseudo-pure-mode qSV-wave equations; e) pseudo-pure-mode scalar qSV-wave field; f) separated scalar qSV-wave field.

Simulation examples of separated scalar qSV-waves

Heterogeneous part of SEG/Hess VTI model

a

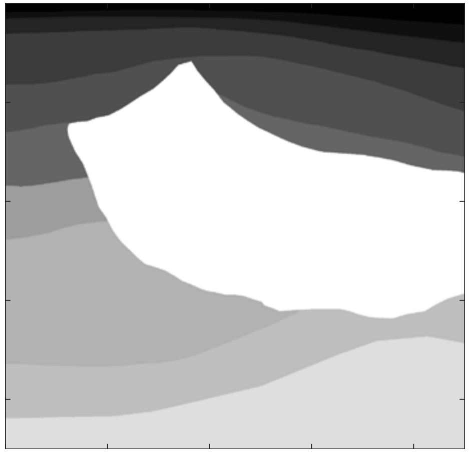

b

FIG. 11. Part of SEG/Hess VTI model: a) C11, b) C13, c) C33 and d) C44.

c

d

For a heterogeneous model, all space-domain deviation operators for each medium need to be calculated with their elastic parameters or Thomsen parameters.

Simulation examples of separated scalar qSV-waves

Heterogeneous part of SEG/Hess VTI model

a

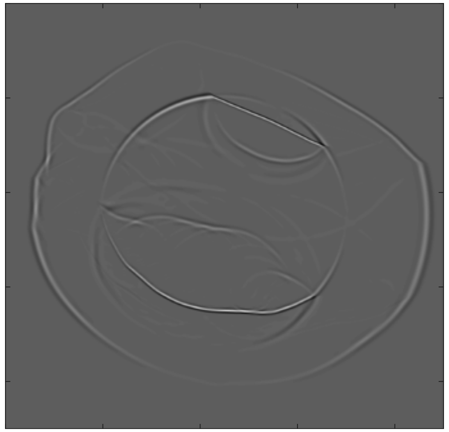

b

c

d

FIG. 12. Synthetic wavefields in SEG/Hess VTI model: a) x- and b) z-component simulated by first-order pseudo-pure-mode qSV-wave equations; c) pseudo-pure-mode scalar qSV-wave field; d) separated scalar qSV-wave field.

Conclusions

- In this study, we have proposed a first-order qSV-wave propagator in general 2D VTI media.
- We have demonstrated this algorithm with synthetic examples of qSV-waves in homogeneous VTI medium with weak/strong anisotropy, layered VTI model and part of SEG/Hess VTI model.
- The snapshots of *x*-component of velocity field propagating at different time demonstrated that first-order Hybrid-PML can be efficiently implemented in this algorithm.
- Similar strategy could be used to develop a qP-wave propagator.

References

- Cheng, J., and Kang, W., 2013, Simulating propagation of separated wave modes in general anisotropic media, part i: qp-wave propagators: Geophysics, 79, No. 1, C1–C18.
- Cheng, J., and Kang, W., 2016, Simulating propagation of separated wave modes in general anisotropic media, part ii: qs-wave propagators: Geophysics, 81, No. 2, C39–C52.
- Liu, H., et al, 2018, A first-order qsv-wave propagator in 2d vti media, in 80th EAGE Conference and Exhibition 2018.
- Thomsen, L., 1986, Weak elastic anisotropy: Geophysics, 51, No. 10, 1954–1966.
- Virieux, J., 1984, SH-wave propagation in heterogeneous media: Velocity-stress finite-difference method: Geophysics, 49, No. 11, 1933–1942.
- Virieux, J., 1986, P-SV wave propagation in heterogeneous media: Velocity-stress finite-difference method: Geophysics, 51, No. 4, 889–901.
- Yan, J., and Sava, P., 2009, Elastic wave-mode separation for vti media: Geophysics, 74, No. 5, WB19–WB32.
- Zhang, J, et al. 2007, P- and S-wave-separated elastic wave-equation numerical modeling using 2D staggered grid. Seg Technical Program Expanded Abstracts. 26. 10.1190/1.2792904.
- Zhang, Q., and McMechan, G. A., 2010, 2d and 3d elastic wavefield vector decomposition in the wavenumber domain for vti media: Geophysics, 75, No. 3, D13–D26.

Acknowledgements

We thank the sponsors of CREWES for continued support. This work was funded by CREWES industrial sponsors, and NSERC (Natural Science and Engineering Research Council of Canada) through the grant CRDPJ 461179-13.